Distributed Multistage Cooperative-Social-Multicast-Aided Content Dissemination in Random Mobile Networks

Jie Hu, *Student Member, IEEE*, Lie-Liang Yang, *Senior Member, IEEE*, and Lajos Hanzo, *Fellow, IEEE*

***Abstract*—A distributed multistage cooperative-social-multicast-protocol-aided content dissemination scheme is proposed, which is based on a self-organized ad hoc network of mobile stations (MSs) seeking the same content. In our content dissemination scheme, upon receiving the content, the content owners may further multicast it to their social contacts who are hitherto unserved content seekers. Then, we mathematically define the geographic social strength to describe the social relationships between a pair of MSs. By jointly considering the geographic social strength, the geographic distances, and the path loss, as well as the small-scale fading, we derive the closed-form formula of the average social unicast throughput. Furthermore, we model the content dissemination process by a discrete-time pure-birth-based Markov chain and derive the closed-form expressions for the statistical properties of the content dissemination delay. The proposed multistage cooperative social multicast protocol is capable of successfully delivering the content of common interest to all MSs in two transmission frames, provided that the density of the MSs is sufficiently high, as demonstrated both by our simulation and analytical results.**

***Index Terms*—Content dissemination, geographic social relationship, multistage cooperative social multicast.**

I. Introduction

IN DENSELY populated areas, such as a football stadium or an open-air festival, mobile users (MUs) always find it difficult to rely on the data services supported by the centralized infrastructure (CI; e.g., Wi-Fi access points and base stations). For instance, in a circular area having a radius of 25 m in one of these scenarios, there may be hundreds of MUs, which may impose a heavy traffic load on the CI. However, the MUs of these particular scenarios usually share the same interest in some of the contents. Based on their multifunctional mobile devices, an ad hoc network can be organized to disseminate the content of common interest via short-range communication techniques, such as Wi-Fi or Bluetooth. As a result, a large fraction of the teletraffic can be offloaded from the CI to the ad hoc network. This promising approach requires for us to design a novel distributed approach for efficiently disseminating the contents of common interest.

As the demand for broadband wireless multimedia services grows, multicast [1] techniques may be invoked to more efficiently disseminate the content of common interest to numerous mobile stations (MSs). Three main types of wireless multicast techniques have attracted attention across the research community [2]–[8]. The first type is the direct wireless multicast [2], where a single node, such as a base station (BS), solely transmits the same content to multiple destinations. In [2], Wang *et al.* theoretically derived both the achievable multicast throughput and delay and then characterized the associated tradeoff between these conflicting performance metrics, while using hybrid-ARQ protocols. To increase the successful content delivery probability, while simultaneously enhancing the coverage area of direct wireless multicast, multihop wireless multicast may be invoked. In this multicast technique, the source node first multicasts the content to all the targets. Then, a specific node is randomly selected from the set of targets who successfully received the content for the sake of further multicasting it to all the other hitherto unserved targets. In [3], Liu and Andrews derived both the outage probability and the multicast transmission capacity for both direct and multihop multicast scenarios. For the sake of further exploiting the diversity gain provided by multiple multicasters, cooperative multicast is proposed for further enhancing the attainable system performance [4]. Given its appealing benefits, substantial efforts have been devoted to the development of two-stage cooperative multicast, particularly to its power allocation [5] and relay selection problems [6]. In two-stage cooperative multicast, the BS first multicasts the content to all the targets. Then, the specific targets who successfully received the content may further multicast it. As a result, the receiver may benefit from a substantial diversity gain, which leads to an improved performance [7]. In [8], Zhao and Su analyzed the outage performance and found the optimal power allocation for both distributed cooperative multicast[1] and for "genie-aided" cooperative multicast.[2] In [9], a social groupcasting algorithm is proposed for a social networking group, so that they become capable of cooperatively downloading the same content

Manuscript received March 7, 2014; revised July 31, 2014; accepted August 28, 2014. This work was supported in part by the Research Council UK's India–UK Advanced Technology Centre (IU-ATC), by the European Union's CONCERTO Project, by the European Research Council's Advanced Fellow Grant, and by the China Scholarship Council (CSC). The review of this paper was coordinated by Dr. L. G. Grieco.

The authors are with the School of Electronics and Computer Science, University of Southampton, Southampton SO17 1BJ, U.K. (e-mail: jh10g11@ecs.soton.ac.uk; lly@ecs.soton.ac.uk; lh@ecs.soton.ac.uk).

Color versions of one or more of the figures in this paper are available online at http://ieeexplore.ieee.org.

Digital Object Identifier 10.1109/TVT.2014.2354295

[1]The second stage of multicast is carried out by MSs who successfully receive the content during the first stage of multicast.

[2]The second stage of multicast is carried out by fixed relay stations.

0018-9545 © 2014 IEEE. Personal use is permitted, but republication/redistribution requires IEEE permission.
See http://www.ieee.org/publications_standards/publications/rights/index.html for more information.

in a heterogeneous network. Unfortunately, Seo *et al.* mainly focused on the scheduling of the content download from the BSs without considering the details of the content dissemination in local ad hoc networks.

However, the aforementioned research efforts ignore the delay analysis of multistage cooperative multicast. Moreover, in self-organized ad hoc networks, the multicasting tasks are carried out by multifunctional mobile handsets, such as smartphones and tablets. Instead of broadcasting the content to all MSs, they usually multicast it to the genuinely interested subset of MSs who are simultaneously their social contacts. These social characteristics of handheld mobile devices are, to a large extent, ignored by the operational wireless systems. Therefore, as argued in [10], it is necessary for us to consider the impact of social networking on the wireless network's performance.

For video sharing in wireless mobile networks, community-based solutions were proposed in [11] and [12], respectively, both of which operated by jointly considering the users' viewing behaviors and their mobility patterns. There is also a growing number of contribution on content dissemination in mobile social networks (MSNs) [13]–[16]. However, these treatises mainly concentrate on large-scale MSNs [17], where the system performance is determined by the encounter properties of mobile nodes. For example, in [16], the continuous-time Markov chain is invoked for analyzing the relevant delay performance, where the state transition rate is determined by the intercontact time between a pair of mobile nodes. This approach cannot be used in small-scale MSNs [17], where the system performance is determined by the wireless channel attenuation and social selection of the targets.[3]

Different from the aforementioned previous works, the novel contributions of this paper are summarized as follows.

1) We propose a novel content dissemination scheme based on a multistage cooperative social multicast protocol for delivering the content of common interest to all the interested MSs in densely populated areas, which falls into the category of small-scale MSNs [17].
2) The social contacts of an MS are categorized into regular contacts and opportunistic contacts based on geographic social relationships.
3) The achievable social unicast throughput is determined by jointly exploiting the social relationships and the wireless links together, and the closed-form expression of the average social unicast throughput is derived.
4) We model the multistage cooperative-social-multicast-protocol-aided content dissemination process by a discrete-time pure-birth-based Markov chain (DT-PBMC) and derive closed-form expressions for characterizing the statistical properties of the content dissemination delay, which is the time when all the MSs successfully receive the content.

[3]In large-scale MSNs, mobile nodes are sparsely distributed over a very large area. Only when a pair of nodes enters each other's transmission range can they communicate. Hence, the system performance is substantially affected by the encounter rate (or the encounter probability) of mobile nodes, by their intercontact time, and by their contact duration. By contrast, in small-scale MSNs, the mobile nodes are densely distributed in a small area, where all pairs of nodes tend to be within each other's transmission range. Hence, the system's performance is mainly affected by a wireless channel, interference, resource allocation, and so on.

TABLE I
NOTATION TABLE

Symbol	Description
N	Number of mobile stations (MSs)
U	Number of initial content owners (COs)
φ	Social Strength
r	Neighbourhood range
α	Social exponent
ν	Packet delivery prob of a wireless link
$h(t)$	Rayleigh distributed fading magnitude
d_0	Reference distance
P_0	Received power at the reference point
κ	Path loss exponent
N_0	Noise power spectrum density
W	Transmission bandwidth
Y	Random distance between a pair of mobile stations
R	Radius of the circular area
$f_Y(y)$	Accurate PDF of the random distance Y
$\widetilde{f_Y}(y)$	Approximate PDF of the random distance Y
K	Random content dissemination delay
$\mathbb{P}(t)$	Random transition matrix
$\mathbf{Q}(t)$	Random transition matrix between transient states
$\mathbf{Q_0}(t)$	Random vector of absorbing probabilities

In the rest of this paper, our content dissemination scheme is first reviewed in Section II. In Section III, we define the geographic social relationships between a pair of MSs, introduce the wireless physical-layer model, and characterize the statistical properties of the geographic distance, followed by the derivation of the closed-form expression for the average social unicast throughput. In Section IV, our content dissemination scheme is modeled by a DT-PBMC to characterize the statistical properties of the content dissemination delay. After presenting both our simulation and analytical results in Section V, we offer our conclusions and a range of potential applications in Section VI. To augment our exposition, we list the important notations in Table I.

II. System Overview

Here, we first introduce the social multicast model, based on which a distributed cooperative-social-multicast-aided content dissemination protocol is proposed. Furthermore, a time-division multiple access (TDMA) approach is invoked for solving the implementation concern of our protocol. Finally, other existing protocols that can be used for content dissemination are introduced.

A. Social Multicast

The basic time unit of our discrete-time system is defined as the duration of a transmission frame. Different from the conventional multicast technique studied in [2]–[8], in this treatise, a content owner (CO) only multicasts the content to the content seekers (CSs) who are simultaneously the CO's social contacts during the current frame.

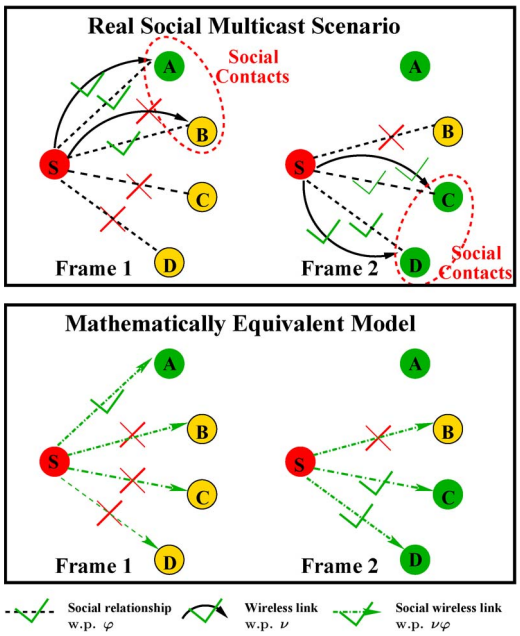

Fig. 1. Example of the social multicast.

The top panel in Fig. 1 portrays a social multicast model in two consecutive frames, where node S represents the CO, whereas nodes A to D represent the CSs. We assume that a CS may be one of the CO's social contacts with a probability of φ. As shown in Fig. 1, during the first frame, nodes A and B are node S's social contacts. Thus, the required physical wireless links are established between S and A as well as between S and B. However, due to the wireless-propagation-induced degradation, a packet is only successfully delivered by a wireless link with a probability of ν. As shown in the top panel in Fig. 1, during the first frame, only the wireless link SA is capable of successfully delivering the content to the target, whereas SB fails. As a result, after the first frame, only node A has received the content successfully. Instead of A and B, nodes C and D become S's social contacts during the second frame. Thus, the required wireless links are established between S and C as well as between S and D. Fortunately, both of these wireless links have successfully delivered the content to the targets. Then, at the end of the second transmission frame, nodes A, C, and D have successfully received the content.

As a result, we observe that the successful packet delivery depends on the following two events: 1) The target is indeed the source's social contact, which occurs with a probability of φ; 2) the physical wireless link successfully delivers the packet from the source to the target, which has a probability of ν. These two independent random events are simultaneously encountered with a probability of $\varphi\nu$. As shown in Fig. 1, to theoretically analyze the content dissemination delay, we may mathematically transform the "Real social multicast scenario" in Fig. 1 into an equivalent model.

Note that in the original social multicast model, S only multicasts the content to its social contacts during each frame. However, in the mathematically equivalent model, S multicasts the content to all the interested CSs via the "social wireless links," which are constituted by a combination of the social relationships and the physical wireless links, as shown in the bottom panel in Fig. 1. Moreover, the probability of a social wireless link successfully delivering a packet of the content to the target is $\varphi\nu$ during a transmission frame. This probability is termed here as the **social unicast throughput**, whose average is derived in Section III.

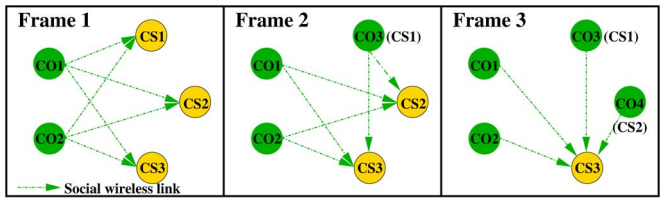

Fig. 2. Multistage cooperative social multicast protocol.

B. Multistage Cooperative Social Multicast Protocol for Content Dissemination

In this treatise, we conceive a multistage cooperative social multicast protocol for disseminating the content of common interest to N MSs, which roam within a bounded circular area. Before the commencement of content dissemination, some MSs actively acquire the content from the CI. These MSs form the initial CO set and cooperatively multicast the content to the other hitherto unserved CSs. The size of this initial CO set is assumed to be U. Once a CS successfully receives the content, it joins the CO set and cooperatively multicasts the content to the other hitherto unserved CSs with the aid of other COs, until all the CSs successfully receive this content. During the content dissemination process, we observe that the size of the CO set continually increases as more and more served CSs join the CO set. If we consider the cooperative action within a specific CO set as a single stage of cooperative social multicast, then we typically need multiple stages of the cooperative social multicast for the sake of completely disseminating the content of common interest to all the CSs.

Fig. 2 portrays an example of the multistage cooperative-social-multicast-aided content dissemination process. During Frame 1, the CO set $\{CO1, CO2\}$ cooperatively multicasts the content to the unserved CS set $\{CS1, CS2, CS3\}$. At the end of Frame 1, $CS1$ successfully receives the content and joins the CO set as $CO3$. Thus, during Frame 2, the new CO set $\{CO1, CO2, CO3\}$ cooperatively multicasts the content to the unserved CS set $\{CS2, CS3\}$. By the end of Frame 2, $CS2$ successfully receives the content and joins the CO set as $CO4$. Finally, during Frame 3, the new CO set $\{CO1, CO2, CO3, CO4\}$ carries out the last stage of cooperative social multicast and successfully delivers the content to the last unserved $CS3$.

C. TDMA Approach For Implementation

According to the protocol introduced in Section II-B, multiple COs simultaneously multicast the content of common interest during a transmission frame. To avoid any collisions

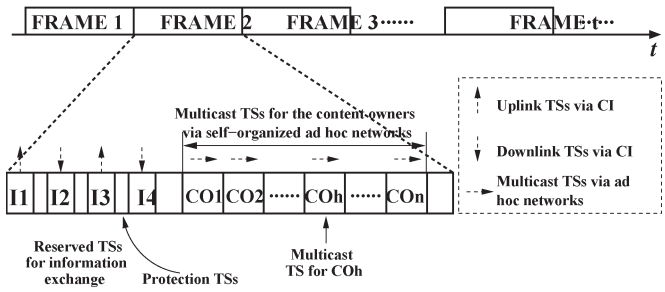

Fig. 3. Frame structure.

incurred by these multiple COs, each CO should be allocated an orthogonal channel. Here, we invoke a TDMA-based approach for implementing our content dissemination scheme.[4] An information controller (IC)[5] is appointed to reduce the overhead of information exchange between COs and CSs. The structure of a transmission frame is shown in Fig. 3.

As shown in Fig. 3, the first four time slots (TSs) are reserved for the side-information exchange between the IC and the COs/CSs. Specifically, the TS "I1" in Fig. 3 is allocated to the COs for reporting their willingness to disseminate the content. The TS "I2" in Fig. 3 is dedicated to the IC for broadcasting both the resource scheduling information and the COs' identities to the potential CSs. The TS "I3" in Fig. 3 is assigned to the active CSs for the sake of reporting their interests to the IC. Moreover, the TS "I4" in Fig. 3 is allocated to the IC for informing the COs of both the active CSs' identities and the resource allocation scheme employed.

Following the information exchange phase, the ad hoc network is ready for content dissemination. As shown in Fig. 3, each CO is allocated a TS for multicasting the content of common interest to its social contacts.

The frame structure portrayed in Fig. 3 is similar to the TDMA scheme proposed in [18] for Wi-Fi mesh networks, where a frame consists of "control slots," "contention slots," and "data slots." The so-called "control slots" in [18] are used both for time synchronization and for explicitly conveying the resource allocation scheme's features and the identities of the mobile nodes. We can see that these "control slots" in [18] have similar functions as those of the TSs reserved for information exchange in our proposed frame structure, as previously introduced. Furthermore, as demonstrated in [18], time synchronization can also be achieved with the aid of "control slots" at high timing accuracy. Nevertheless, due to the IC, accurate time synchronization can be more readily realized in our TDMA approach than in the distributed approach in [18]. Moreover, as reported in [18], the control overhead is less than 10% for a purely self-organized ad hoc network operating without any ICs. Hence, with the aid of the IC, we impose an even lower control overhead in our scheme.

[4]Other approaches that are capable of providing orthogonal channels can also be implemented, such as carrier-sense multiple access, orthogonal frequency-division multiple access, and code-division multiple access.

[5]CI, such as a BS and a Wi-Fi access point, is a nature-born IC, since all the MSs in the same area regularly exchange pilots with it.

D. Other Protocols for Content Dissemination

There are other protocols for content dissemination in literatures. To implement these protocols in our model, we should impose the social constraints that a transmitter is only willing to unicast/multicast the content to its social contacts on these existing protocols.

1) Noncooperative Direct Social Multicast (Noncoop Direct So-Multicast): This protocol originates from the conventional direct multicast, which was studied in [2]. Although we may have multiple COs at the beginning, in this protocol, we assume that there is only a single CO, who continually multicasts the content of common interest to its social contacts, until all the other unserved CSs successfully receive it, as detailed in Section II-A. The social multicast delay of this protocol has been characterized in our previous work [19].

2) Single-Stage Cooperative Social Multicast (Single-Stage Coop So-Multicast): This protocol originates from the widely studied cooperative multicast model in [4]–[8], where only those specific COs that initially own the content would cooperatively multicast the content to their social contacts.

3) Noncooperative Gossip-Based Social Unicast (Noncoop Gossip So-Unicast): This protocol originates from [20] and was further invoked for information dissemination in [21]. When we implement this protocol in our scenario, we made a few changes in comparison to the protocol studied in [21]. During a transmission frame, a CO may have several social contacts, and it has to select a single social contact from its social contacts to form a CO and CS pair for further disseminating the content. If a CS has already been selected by one of the COs, it cannot be selected by other COs. According to [21], for the sake of forming this CO and CS pair, the CS should be randomly selected from the CO's social contacts. However, to form as many CO and CS pairs as possible, in our algorithm, a CO that has fewer social contacts during a transmission frame has a higher priority to select a CS, who is simultaneously one of the CO's social contact. After the CS successfully receives the content, it may join the set of COs for futher disseminating the content.

III. Social Unicast Throughput of a Social Wireless Link

Here, we will first define the probability φ that a CS becomes a CO's social contact, while deriving the successful packet reception probability ν of a physical wireless link. Then, we derive the closed-form formula for the average social unicast throughput.

A. Geographic Social Relationships

In Milgram's widely known "small world" experiment [22], he proved that there was a maximum of six-hop separation, on average, between any pair of people in the United States. Furthermore, Watts and Strogatz claimed that any network obeys a hybrid structure between regular networks and random networks [23]. They also defined the so-called short-range

and long-range contacts. The well-known results of Milgram's experiment were theoretically proved in [24] and [25].

Kleinberg in [26] studied a 2-D grid network obeying the small-world property in [23]. In [26], source node s selects any other node v as its long-range contact with a probability proportional to $y^{-\alpha}(s,v)$, where $y(s,v)$ is the distance between s and v, whereas α is a social exponent. Here, the 'distance' may indicate either a virtual social distance or an exact geographic distance. This work was extended to wireless ad hoc networks in [27] to analyze the impact of social groups on the wireless network's capacity, where a node in the wireless ad hoc network is selected to be the target with a probability proportional to $y^{-\alpha}(s,v)$, where $y(s,v)$ represents the exact geographic distance.

Furthermore, Liben-Nowell *et al.* in [28] found that when the geographic distance is shorter than 1000 km, the probability of a pair of users sharing a social relationship largely depends on the geographic distance between them.[6] This probability is proportional to $y^{-\alpha}$, where the social exponent α is estimated to be 1.2. Similar results were also provided in [29], where the social exponent was estimated for mobile communication. When using the maximum-likelihood method in [30], these exponents were found to be $\alpha \approx 1.58$ for voice ties and $\alpha \approx 1.49$ for text ties.

Based on the aforementioned literature, we assume that if a CS is within the neighborhood range of a CO, the probability of this CS becoming the CO's social contact is unity, and this CS is termed as the *regular contact* of the CO. If the CS is beyond the neighborhood range of the CO, the CS may still become the social contact of the CO with a probability that is inversely proportional to the geographic distance between them. This sort of social contact is termed as opportunistic contact. As a result, the probability of a CS becoming a CO's social contact,[7] which is also termed as social strength, is defined as

$$\varphi|_{Y=y} = \begin{cases} 1, & 0 \le y \le r \\ \frac{1}{\left(\frac{y}{r}\right)^{\alpha}}, & y > r \end{cases} \tag{1}$$

where y is the geographic distance between a pair of MSs, r is the neighborhood range, and α is the social exponent in line with [26]–[29].

In Fig. 4, eight nodes are seen to be uniformly arranged on a circle. If $\alpha = +\infty$, indicating that a node only has regular contacts (solid lines in Fig. 4), as r increases from l to $4l$, a node may have more regular contacts for potential communications. If we fix r to l, indicating that a node only has the adjacent nodes in its regular contact set, as α reduces from infinity to 0, in line with (1), a node may have more opportunistic contacts (dotted lines in Fig. 4).

[6]The data are extracted from an online community—LiveJournal (http://www.livejournal.com).

[7]For the sake of social contact selection, a CO should be aware of the distances from itself to CSs. This distance awareness can be easily realized by the GPS module and the relevant mobile applications (such as WeChat: http://www.wechat.com) installed on the CO's multifunctional mobile devices.

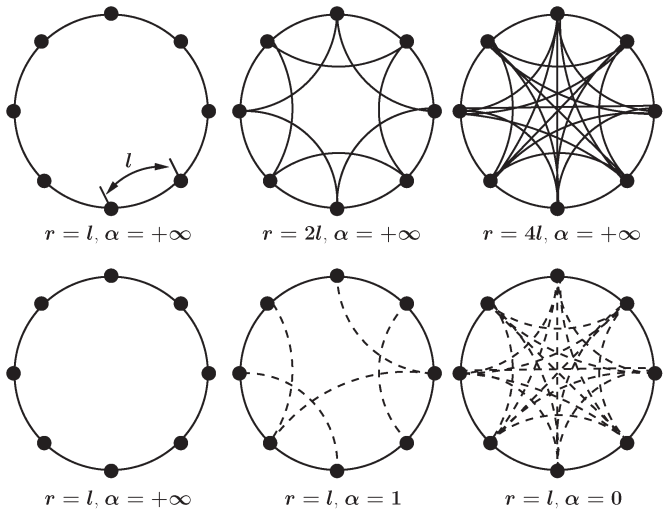

Fig. 4. Impact of the neighborhood range and social exponent on social relationships.

B. Successful Packet Delivery Probability of a Physical Wireless Link

1) Small-Scale Fading: The small-scale fading is modeled by uncorrelated stationary flat Rayleigh fading [31]. The fading magnitude $|h(t)|$ during the tth TS, which varies from one TS to another, is a Rayleigh distributed random variable. Since each CO is assigned a single TS during a transmission frame according to Section II-B, t can also be interpreted as the index of the frame. Consequently, the square of the channel's magnitude $|h(t)|^2$ obeys the exponential distribution associated with $E[|h(t)|^2] = 1$. The probability density function (pdf) and the cumulative distribution function (cdf) of $X = |h(t)|^2$ are $f_X(x) = \exp(-x)$ and $F_X(x) = 1 - \exp(-x)$, $x > 0$, respectively.

2) PL: According to [31], the path loss (PL) equation is invalid for calculating the attenuation in the near-field of the transmit antennas. We assume that the PL only imposes attenuation on a wireless link, when its length y is longer than a reference threshold d_0. Then, the PL model is formulated as

$$\frac{P_r}{P_0} = \begin{cases} 1, & 0 \le y \le d_0 \\ \frac{1}{\left(\frac{y}{d_0}\right)^{\kappa}}, & y > d_0 \end{cases} \tag{2}$$

where P_0 is the received power at the point that is d_0 m away from the transmitter and P_r is the power received after experiencing PL at a CS, whereas κ is the PL exponent.

3) Successful Packet Delivery: In the MAC layer, we assume that a packet of the content is successfully transmitted during a TS from a CO to a CS, only when the instantaneous received signal-to-noise ratio (SNR) is above a predefined threshold γ [32]. As a result, when jointly considering the small-scale fading and the PL, the successful packet delivery probability of a physical wireless link is given by

$$\nu|_{Y=y} = \begin{cases} P\left(|h|^2 > Ad_0^{\kappa}\right) = e^{-Ad_0^{\kappa}}, & 0 \le y \le d_0 \\ P\left(|h|^2 > Ay^{\kappa}\right) = e^{-Ay^{\kappa}}, & y > d_0 \end{cases} \tag{3}$$

where we have $A = (\gamma N_0 W)/(P_0 d_0^{\kappa})$, and y is the distance between a CO and CS pair, whereas $N_0 W$ is the noise power. Naturally, $\nu|_{Y=y}$ is equivalent to the throughput of the physical wireless link expressed in packets per frame [33].

C. PDF of the Random Geographic Distance

1) Mobility and Connectivity: We assume that all MSs roam in a bounded circular area having a radius of R. The position of the ith MS during frame t is denoted by $\mathbf{P}_i(t)$, which obeys a stationary and ergodic process with a stationary uniform distribution in the circular area [34]. Moreover, the positions of different MSs are independent and identically distributed (i.i.d.). This mobility model has been widely used for analyzing the performance of mobile networks [21].

Moreover, the range of Wi-Fi in outdoor scenarios can be up to 100 m. If the diameter of the studied circular area is shorter than this range, it is reasonable for us to assume that CSs are always in the transmission range of COs. Hence, our model belongs to the scenario of small-scale MSNs [17], where the system performance is dominated by the wireless channel's attenuation and the specific social contact selection.

2) PDF of the Geographic Distance: We may derive the pdf of the geographic distance Y between a pair of MSs by exploiting the following methodology. Given that the source is currently located at a point $\mathbf{P} = \mathbf{p}$, we may derive the conditional probability $P(Y \le y|\mathbf{P} = \mathbf{p})$ by computing the intersection area of two circles, one of which is the considered circular area, and the other is a circle centered at the point $\mathbf{P} = \mathbf{p}$ having a radius of y. Integrating $P(Y \le y|\mathbf{P} = \mathbf{p})$ over all possible points gives us the cdf of Y, whose derivative gives the pdf of Y between a pair of MSs [35], i.e.,

$$f_Y(y) = \frac{8}{\pi R}\frac{y}{2R}\left[\arccos\left(\frac{y}{2R}\right) - \frac{y}{2R}\sqrt{1-\left(\frac{y}{2R}\right)^2}\right] \quad (4)$$

for $0 \le y \le 2R$, and 0, otherwise.

However, due to its complexity, further integration over $f_Y(y)$ may not produce a closed-form expression. Hence, we may need an approximate alternative expression for $f_Y(y)$. Given the following two Taylor-expansion-based expressions:

$$\arccos(z) = \frac{\pi}{2} - \sum_{n=0}^{\infty}\frac{(2n)!}{4^n(n!)^2(2n+1)}\cdot z^{2n+1} \quad (5)$$

$$\sqrt{1-z^2} = 1 + \sum_{n=1}^{\infty}\prod_{m=1}^{n}(2m-3)\frac{z^{2n+1}}{n!2^n} \quad (6)$$

by replacing z in (6) with $y/2R$ and substituting them into (4), we arrive at an alternative expression for (4), i.e.,

$$f_Y(y) = \frac{8}{\pi R}\left[\frac{\pi}{2}\frac{y}{2R} + \sum_{n=0}^{\infty}C_n\left(\frac{y}{2R}\right)^{2n+2}\right] \quad (7)$$

$$\text{where } C_n = \frac{2\cdot(2n)!}{4^n(n!)^2(2n+1)(2n-1)} \quad (8)$$

for $0 \le y \le 2R$, and 0, otherwise.

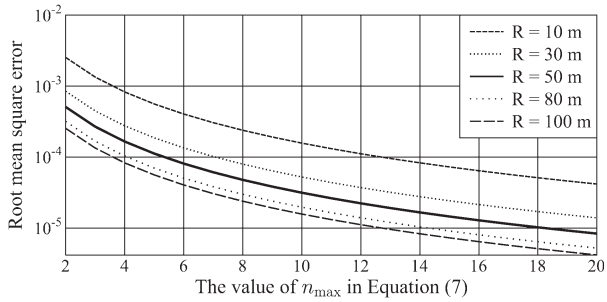

Fig. 5. RMSE between $\widetilde{f_Y}(y)$ and $f_Y(y)$.

If we limit the maximum number of terms in the summation to $n_{\max}$, we arrive at an approximate version of (7), i.e.,

$$\widetilde{f_Y}(y) = C_Y\cdot\frac{8}{\pi R}\left(\frac{\pi}{2}\frac{y}{2R} + \sum_{n=0}^{n_{\max}}C_n\left(\frac{y}{2R}\right)^{2n+2}\right) \quad (9)$$

$$\text{where } C_Y = \frac{\pi}{4}\left(\pi + \sum_{n=0}^{n_{\max}}\frac{4C_n}{2n+3}\right)^{-1} \quad (10)$$

for $0 \le y \le 2R$, and 0, otherwise. The constant C_Y in (9) is derived for the sake of guaranteeing that $\int_0^{2R}\widetilde{f_Y}(y)dy = 1$.

In Fig. 5, we plot the root-mean-square error (RMSE) between $f_Y(y)$ of (4) and $\widetilde{f_Y}(y)$ of (9). As shown in Fig. 5, when R is higher than 10 m, $n_{\max} = 4$ guarantees that the RMSE becomes lower than 10^{-3}. This sufficiently low RMSE indicates that our approximation is valid for most practical cases.

D. Analysis of the Social Unicast Throughput

Given a specific distance of $Y = y$, we denote the social unicast throughput as $\mu|_{Y=y} = \varphi|_{Y=y}\cdot\nu|_{Y=y}$. Then, we may derive the average social unicast throughput by integrating $\mu|_{Y=y}$ over all possible values of $Y = y$. However, we may have different expressions for $\mu|_{Y=y}$, given the different values of the neighborhood range r and PL reference distance d_0 as follows.

Case 1: If $d_0 \le r$, then we have the following expression for $\mu_{(1)}^m|_{Y=y}$:

$$\mu_{(1)}|_{Y=y} = \begin{cases} e^{-Ad_0^{\kappa}}, & 0 \le y \le d_0 \\ e^{-Ay^{\kappa}}, & d_0 < y \le r \\ e^{-Ay^{\kappa}}\cdot\left(\frac{y}{r}\right)^{-\alpha}, & r < y \le 2R. \end{cases} \quad (11)$$

Therefore, the mth moment of the social unicast throughput can be formulated as

$$E\left[\mu_{(1)}\right] = \underbrace{\int_0^{d_0} e^{-Ad_0^{\kappa}} f_Y(y)\,dy}_{I_1^{(1)}} + \underbrace{\int_{d_0}^{r} e^{-Ay^{\kappa}} f_Y(y)\,dy}_{I_2^{(1)}} + \underbrace{\int_r^{2R} e^{-Ay^{\kappa}}\left(\frac{r}{y}\right)^{\alpha} f_Y(y)\,dy}_{I_3^{(1)}}. \quad (12)$$

Let us now substitute $f_Y(y)$ of (4) into the first integral $I_1^{(1)}$ of (12). Hence, $I_1^{(1)}$ can be formulated as

$$\begin{aligned} I_1^{(1)} &= \int_0^{d_0} e^{-Ad_0^\kappa} f_Y(y)\, dy \\ &= e^{-Ad_0^\kappa} \cdot \frac{2}{\pi} \left\{ 4\left(\frac{y}{2R}\right)^2 \arccos\left(\frac{y}{2R}\right) + \arcsin\left(\frac{y}{2R}\right) \right. \\ &\quad \left. - \left[\frac{y}{2R} + 2\left(\frac{y}{2R}\right)^3\right] \sqrt{1-\left(\frac{y}{2R}\right)^2} \right\} \Bigg|_0^{d_0}. \end{aligned} \tag{13}$$

Given the inherent complexity of (4), we have to substitute the approximate pdf $\widetilde{f_Y}(y)$ of (9) into $I_2^{(1)}$ of (12), we have

$$\begin{aligned} I_2^{(1)} &\approx \int_{d_0}^{r} e^{-Ay^\kappa} \widetilde{f}_Y(y)\, dy \\ &= \int_{d_0}^{r} e^{-Ay^\kappa} \cdot \frac{8C_Y}{\pi R} \left(\frac{\pi}{2} \frac{y}{2R} + \sum_{n=0}^{n_{\max}} C_n \left(\frac{y}{2R}\right)^{2n+2} \right) dy \\ &= \frac{8C_Y}{\pi R} \left[\frac{\pi}{4R} \int_{d_0}^{r} e^{-Ay^\kappa} y\, dy + \sum_{n=0}^{n_{\max}} \right. \\ &\quad \left. \times \frac{C_n}{(2R)^{2n+2}} \int_{d_0}^{r} e^{-Ay^\kappa} y^{2n+2}\, dy \right] \\ &= \frac{8C_Y}{\pi R} \left[\frac{\pi}{4R} \Phi(y|1,0,A) + \sum_{n=0}^{n_{\max}} \frac{C_n \Phi(y|2n+2,0,A)}{(2R)^{2n+2}} \right] \Bigg|_{d_0}^{r} \end{aligned} \tag{14}$$

where the function $\Phi(y|\beta,\alpha,A)$ is defined as

$$\begin{aligned} \Phi(y|\beta,\alpha,A) &= \int y^{\beta-\alpha} e^{-Ay^\kappa} dy \\ &= \begin{cases} -\frac{A^{z_1}\Gamma(-z_1, Ay^\kappa)}{\kappa}, & z_1 = \frac{\alpha-\beta-1}{\kappa}, \quad \text{if } \beta < \alpha \\ -\frac{\Gamma(z_2, Ay^\kappa)}{\kappa A^{z_2}}, & z_2 = \frac{\beta-\alpha+1}{\kappa}, \quad \text{if } \beta \geq \alpha \end{cases} \end{aligned} \tag{15}$$

while functions $\Gamma(-z_1, Ay^\kappa)$ and $\Gamma(z_2, Ay^\kappa)$ are given by the following two equations [36]:

$$\Gamma(-z_1, Ay^\kappa) = \int_{Ay^\kappa}^{\infty} \frac{1}{t^{z_1+1}} e^{-t} dt, \Gamma(z_2, Ay^\kappa) = \int_{Ay^\kappa}^{\infty} t^{z_2-1} e^{-t} dt.$$

Furthermore, the closed-form expression for the third integral $I_3^{(1)}$ of (12) can also be derived by substituting $\widetilde{f_Y}(y)$ of (9) into $I_3^{(1)}$, which is expressed as

$$\begin{aligned} I_3^{(1)} &\approx \int_r^{2R} e^{-Ay^\kappa} \left(\frac{r}{y}\right)^\alpha \widetilde{f_Y}(y) dy \\ &= \int_r^{2R} e^{-Ay^\kappa} \left(\frac{r}{y}\right)^\alpha \frac{8C_Y}{\pi R} \left(\frac{\pi}{2} \frac{y}{2R} + \sum_{n=0}^{n_{\max}} C_n \left(\frac{y}{2R}\right)^{2n+2} \right) dy \\ &= \frac{8C_Y r^\alpha}{\pi R} \left[\frac{\pi}{4R} \Phi(y|1,\alpha,A) \right. \\ &\quad \left. + \sum_{n=0}^{n_{\max}} \frac{C_n \Phi(y|2n+2,\alpha,A)}{(2R)^{2n+2}} \right] \Bigg|_r^{2R} \end{aligned} \tag{16}$$

where function $\Phi(y|\beta,\alpha,A)$ has been defined in (15).

Case 2: If $d_0 > r$, then we have the following expression for $\mu_{(2)}^m|_{Y=y}$:

$$\mu_{(2)}|_{Y=y} = \begin{cases} e^{-Ad_0^\kappa}, & 0 \leq y \leq r \\ e^{-Ad_0^\kappa} \cdot \left(\frac{y}{r}\right)^{-\alpha}, & r < y \leq d_0 \\ e^{-Ay^\kappa} \cdot \left(\frac{y}{r}\right)^{-\alpha}, & d_0 < y \leq 2R. \end{cases} \tag{17}$$

Similarly to (12), we may express the average social unicast throughput as

$$\begin{aligned} E\left[\mu_{(2)}\right] &= \underbrace{\int_0^r e^{-Ad_0^\kappa} f_Y(y)\, dy}_{I_1^{(2)}} + \underbrace{\int_r^{d_0} e^{-Ad_0^\kappa} \left(\frac{r}{y}\right)^\alpha f_Y(y)\, dy}_{I_2^{(2)}} \\ &\quad + \underbrace{\int_{d_0}^{2R} e^{-Ay^\kappa} \left(\frac{r}{y}\right)^\alpha f_Y(y)\, dy}_{I_3^{(2)}}. \end{aligned} \tag{18}$$

Substituting the integration limits of $[0, d_0]$ in (13) by $[0, r]$, we are now capable of deriving the closed-form formula for $I_1^{(2)}$. Similarly, substituting the integration limits of $[r, 2R]$ in (16) by $[d_0, 2R]$, we arrive at the closed-form formula for $I_3^{(2)}$. However, we have to derive the integral $I_2^{(2)}$ specifically. Substituting $\widetilde{f_Y}(y)$ of (9) into $I_2^{(2)}$ of (18), $I_2^{(2)}$ is expressed as

$$\begin{aligned} I_2^{(2)} &\approx \int_r^{d_0} e^{-Ad_0^\kappa} \left(\frac{r}{y}\right)^\alpha \widetilde{f_Y}(y)\, dy \\ &= \int_r^{d_0} e^{-Ad_0^\kappa} \left(\frac{r}{y}\right)^\alpha \frac{8C_Y}{\pi R} \left(\frac{\pi}{2} \frac{y}{2R} + \sum_{n=0}^{n_{\max}} C_n \left(\frac{y}{2R}\right)^{2n+2} \right) dy \\ &= e^{-Ad_0^\kappa} \cdot \frac{8C_Y r^\alpha}{\pi R} \left[\frac{\pi}{4R} \int_r^{d_0} y^{1-\alpha}\, dy \right. \\ &\quad \left. + \sum_{n=0}^{n_{\max}} \frac{C_n}{(2R)^{2n+2}} \int_r^{d_0} y^{2n+2-\alpha} dy \right] \end{aligned}$$

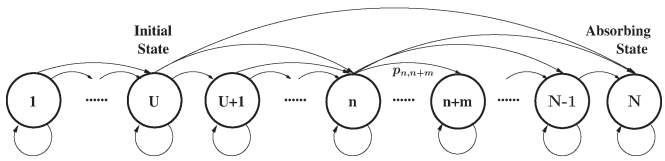

Fig. 6. DT-PBMC.

$$=e^{-Ad_0^{\kappa}}\cdot\frac{8C_Y r^{\alpha}}{\pi R}\left[\frac{\pi}{4R}\Psi(y|1,\alpha)+\sum_{n=0}^{n_{\max}}\frac{C_n}{(2R)^{2n+2}}\Psi(y|2n+2,\alpha)\right]\Bigg|_r^{d_0} \tag{19}$$

where function $\Psi(y|\beta,\alpha)$ is defined as

$$\Psi(y|\beta,\alpha)=\int y^{\beta-\alpha}dy=\begin{cases}\frac{y^{\beta-\alpha+1}}{\beta-\alpha+1}, & \text{if } \beta-\alpha\neq -1\\ \ln y, & \text{if } \beta-\alpha=-1.\end{cases} \tag{20}$$

In a nutshell, the average social unicast throughput is obtained as

$$\overline{\mu}=E[\mu]=\begin{cases}I_1^{(1)}+I_2^{(1)}+I_3^{(1)}, & \text{if } d_0\le r\\ I_1^{(2)}+I_2^{(2)}+I_3^{(2)}, & \text{if } d_0>r.\end{cases} \tag{21}$$

IV. Delay Analysis of Cooperative-Social-Multicast-Aided Content Dissemination

Let us now analyze the delay characteristics of the multistage cooperative-social-multicast-protocol-aided content dissemination.

A. DT-PBMC

According to Section II-B, all the CSs become the COs upon successfully receiving the content of common interest. Hence, the number of the COs increases, until all the N MSs in this area receive the content. Hence, we model this multistage cooperative-social-multicast-protocol-aided content dissemination process by a DT-PBMC, as shown in Fig. 6.

State n of the DT-PBMC represents the number of COs during the current frame, whereas the number of unserved CSs is $(N-n)$. Observe in Fig. 6 that $p_{n,n+m}$ $(m\ge 0)$ represents the probability of the DT-PBMC's transition from state n to state $(n+m)$ during this transmission frame, which also indicates the probability of m unserved CSs out of $(N-n)$ successfully receiving the content. When we have $m=0$, the state transition probability $p_{n,n}$ represents the fact that no unserved CS receives the content during the current frame. As shown in Fig. 6, the state transitions emerge from the initial state U $(1\le U<N)$, where U represents the number of initial COs before the content dissemination according to Section II-A, and terminate at the absorbing state N, which is the total number of MSs in the area. All the other states between the initial state U and the absorbing state N are termed as transient states. Since the content dissemination is a discrete-time process,[8] the content dissemination delay K is equivalent to the number of transmission frames, when the absorbing state N is reached after emerging from the initial state U.

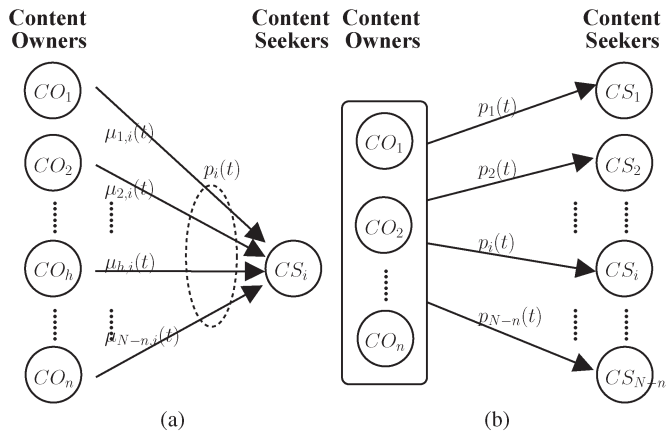

Fig. 7. Content dissemination in a frame. (a) Packet reception at a CS. (b) Equivalent social multicast.

Before delving into the statistical properties of the random content dissemination delay K, we first have to derive the state transition probability $p_{n,n+m}$ and the state transition matrix $\mathbb{P}$.

B. State Transition Matrix

1) Successful Packet Reception Probability of a CS: According to the frame structure in Fig. 3, at the beginning of the tth frame, n TSs are allocated to COs, if there are n COs willing to multicast the content to the $(N-n)$ unserved CSs. Specifically, the hth TS during the tth frame is allocated to CO_h $(1\le h\le n)$. As shown in Fig. 7(a), CS_i $(1\le i\le N-n)$ is connected to all the COs via the "social wireless link" defined in Section II-A. Moreover, the successful packet delivery probability of the "social wireless link" connecting CO_h and CS_i is equivalent to the social unicast throughput $\mu_{h,i}(t)$.

According to Figs. 3 and 7(a), the packet detection process of CS_i is characterized as follows. In each frame, CS_i detects the signal of the n multicast TSs one by one to successfully receive a packet. If the packet is indeed successfully detected during the hth TS, the detection process is terminated. By contrast, if the packet cannot be detected in any of the n multicast TSs, the detection process is terminated, and the unserved CS_i will request the content again during the next frame. As a result, during the transmission of the tth frame, the probability of CS_i successfully detecting a packet within the hth multicast TS, which implies that the packet's detection failed during the first $(h-1)$ TSs, is expressed as

$$p_i^{(h)}(t)=\prod_{j=1}^{h-1}\left[1-\mu_{j,i}(t)\right]\cdot\mu_{h,i}(t) \tag{22}$$

[8] As defined at the beginning of Section II-A, the basic time unit in this discrete-time system is the duration of a transmission frame.

where $\mu_{j,i}(t)$ is the social unicast throughput of the "social wireless link" connecting CO_j and CS_i during the dissemination of the tth frame. Since the social unicast throughput $\mu_{j,i}(t)$ is determined by the time-varying geographic distance and by small-scale fading, they may be assumed to remain constant during the tth frame, but they independently vary from one frame to another.

As a result, the probability of CS_i successfully receiving a packet during the tth frame is formulated as

$$p_i(t) = \sum_{h=1}^{n} p_i^{(h)}(t) = \sum_{h=1}^{n} \prod_{j=1}^{h-1} [1 - \mu_{j,i}(t)] \cdot \mu_{h,i}(t)$$
$$= 1 - \prod_{h=1}^{n} [1 - \mu_{h,i}(t)]. \quad (23)$$

According to the mobility model introduced in Section III-C, the geographic positions of different MSs are i.i.d. random variables; thus, the distances between any CO and CS pair are also i.i.d. random variables. Hence, according to (11) and (17), $\{\mu_{h,i}(t), h = 1, 2, \ldots, n\}$ are also i.i.d. random variables. As a result, the expected value of $p_i(t)$ may be expressed as

$$\overline{p} = E[p_i(t)] = 1 - \prod_{h=1}^{n} (1 - E[\mu_{h,i}(t)]) = 1 - (1 - \overline{\mu})^n \quad (24)$$

where $\overline{\mu}$ is the average social unicast throughput that is derived in Section III-D.

2) State Transition Probability: Fig. 7(b) portrays the cooperative-multicast-aided content dissemination process during the tth frame, given n COs and $(N - n)$ CSs, where $p_i(t)$ of (23) is the probability of CS_i successfully receiving a packet of the content during the tth frame.

Let us assume that m CSs having indexes of $\mathcal{I} = \{i_g | 1 \leq g \leq m\}$ receive the packet at the end of the current frame associated with the successful packet reception probabilities of $\mathcal{P}_{\mathcal{I}} = \{p_{i_g}(t) | i_g \in \mathcal{I}\}$, whereas the remaining $(N - n - m)$ CSs having indexes of $\mathcal{J} = \{j_h | 1 \leq h \leq (N - n - m)\}$ do not receive any packets. The latter event is associated with the unsuccessful packet reception probabilities of $\mathcal{P}_{\mathcal{J}} = \{1 - p_{j_h}(t) | j_h \in \mathcal{J}\}$. We should note that $\mathcal{I} \bigcap \mathcal{J} = \phi$, whereas $\mathcal{I} \bigcup \mathcal{J}$ is the full set of $(N - n)$ unserved CSs at the beginning of the current frame. Furthermore, $\mathcal{P}_{\mathcal{I}}$ and $\mathcal{P}_{\mathcal{J}}$ are independent of each other. Thus, the state transition probability $p_{n,n+m}$ may be expressed as

$$p_{n,n+m}(t) = \sum_{\text{All possible combinations for } \mathcal{I}} \times \left[\prod_{i_g \in \mathcal{I}} p_{i_g}(t) \prod_{j_h \in \mathcal{J}} (1 - p_{j_h}(t)) \right]. \quad (25)$$

As a result, the $(N \times N)$-element state transition matrix $\mathbb{P}(t)$ of the DT-PBMC during the tth frame is expressed as (26), shown at the bottom of the page, where $\mathbf{Q}(t)$ is the $(N-1) \times (N-1)$-element transition matrix for the $(N-1)$ transient states of the DT-PBMC, and $\mathbf{Q_0}(t)$ is the $(N-1) \times 1$-element vector consisting of the probabilities of the transient states being absorbed.

Since the entries of $\mathbb{P}(t)$ are random variables, $\mathbb{P}(t)$ is a random matrix. Taking the expected value of every entry in $\mathbb{P}(t)$, the expected matrix of $\mathbb{P}(t)$ is formulated as

$$\overline{\mathbb{P}} = E[\mathbb{P}(t)] = \begin{pmatrix} \overline{\mathbf{Q}} & \overline{\mathbf{Q}}_0 \\ \mathbf{0} & 1 \end{pmatrix}. \quad (27)$$

Given $p_{n,n+m}(t)$ derived in (25) and that all the elements in $\mathcal{P}_{\mathcal{I}}$ are i.i.d. random variables having an identical mean of $\overline{p}$ as well as that all the elements in $\mathcal{P}_{\mathcal{J}}$ are i.i.d. random variables having an identical mean of $(1 - \overline{p})$, the associated entry $\overline{p_{n,n+m}}$ of $\overline{\mathbb{P}}$ becomes

$$\overline{p_{n,n+m}} = \sum_{\text{All possible combination for } \mathcal{I}} \times \left[\prod_{i_g \in \mathcal{I}} E[p_{i_g}(t)] \prod_{j_h \in \mathcal{J}} E[1 - p_{j_h}(t)] \right]$$
$$= \binom{N-n}{m} \overline{p}^m (1-\overline{p})^{N-n-m}$$
$$= \binom{N-n}{m} (1-(1-\overline{\mu})^n)^m (1-\overline{\mu})^{n(N-n-m)} \quad (28)$$

where the third equality is obtained by substituting (24) into (28).

$$\mathbb{P}(t) = \begin{pmatrix} p_{1,1}(t) & p_{1,2}(t) & p_{1,3}(t) & p_{1,4}(t) & \cdots & p_{1,N-1}(t) & p_{1,N}(t) \\ 0 & p_{2,2}(t) & p_{2,3}(t) & p_{2,4}(t) & \cdots & p_{2,N-1}(t) & p_{2,N}(t) \\ \vdots & \vdots & \ddots & \vdots & & \vdots & \vdots \\ 0 & 0 & \cdots & p_{U,U}(t) & \cdots & p_{U,N-1}(t) & p_{U,N}(t) \\ \vdots & \vdots & & & \ddots & \vdots & \vdots \\ 0 & 0 & \cdots & 0 & \cdots & p_{N-1,N-1}(t) & p_{N-1,N}(t) \\ 0 & 0 & \cdots & 0 & \cdots & 0 & p_{N,N}(t) \end{pmatrix}$$
$$= \begin{pmatrix} \mathbf{Q}(t) & \mathbf{Q_0}(t) \\ \mathbf{0} & 1 \end{pmatrix} \quad (26)$$

C. Statistical Properties of the Content Dissemination Delay

To derive the tail distribution function (tdf) of the content dissemination delay and its average value, we only have to consider the transition matrix of the transient states, which is denoted by $\mathbf{Q}(t)$ in (26). Specifically, we have $\mathbf{Q}(0)=\mathbf{I}$, indicating that the DT-PBMC has a unity probability of staying in its current state.

Theorem 1: The entry $q_{i,j}(k)$ of the matrix $\mathbb{Q}(k)=\prod_{t=0}^{k}\mathbf{Q}(t)$ represents the probability of state j being reached after k frames, given that the initial state is state i.

Proof: See Appendix A. ■

Before deriving the statistical properties of the content dissemination delay, we must first study the convergence of matrix $\mathbb{Q}(k)$. As a result, Theorem 2 is formulated.

Theorem 2: Given $\mathbb{Q}(k)=\prod_{t=0}^{k}\mathbf{Q}(t)$, when k tends to infinity, we have $\mathbb{Q}(k)\to\mathbf{0}$, as well as $E[\mathbb{Q}(k)]=\overline{\mathbf{Q}}^{k}\to\mathbf{0}$.

Proof: See Appendix B. ■

With the aid of Theorem 1 and Theorem 2, we obtain matrix $\mathbb{Q}(k)$ containing the probabilities of any transient states being reached from any initial states after k frames.

Given the initial state i, the probability of the DT-PBMC not being terminated after k frames is the sum of the entries in row i of matrix $\mathbb{Q}(k)$, which is also the probability of the random content dissemination delay K being larger than k. The initial state of content dissemination is set to U, according to Section IV-A. Hence, the conditional tdf of the content dissemination delay is

$$P\left[K>k|\mathbb{Q}(k)\right]=\overrightarrow{\boldsymbol{\tau}}\mathbb{Q}(k)\overrightarrow{\mathbf{1}} \tag{29}$$

where $\overrightarrow{\boldsymbol{\tau}}$ is a $1\times(N-1)$-element row vector, whose Uth entry is one and all the other entries are zero, $\overrightarrow{\mathbf{1}}$ is an $(N-1)\times 1$-element column vector, whose entries are all one. According to the Bayesian principle and Theorem 2, the tdf of the content dissemination delay can be expressed as

$$\begin{aligned}P(K>k)&=\int_{\mathbb{Q}(k)}P\left[K>k|\mathbb{Q}(k)\right]f\left[\mathbb{Q}(k)\right]d\mathbb{Q}(k)\\&=\overrightarrow{\boldsymbol{\tau}}\times\int_{\mathbb{Q}(k)}\mathbb{Q}(k)f\left[\mathbb{Q}(k)\right]d\mathbb{Q}(k)\times\overrightarrow{\mathbf{1}}\\&=\overrightarrow{\boldsymbol{\tau}}E\left[\mathbb{Q}(k)\right]\overrightarrow{\mathbf{1}}=\overrightarrow{\boldsymbol{\tau}}\overline{\mathbf{Q}}^{k}\overrightarrow{\mathbf{1}}\end{aligned} \tag{30}$$

where $f[\mathbb{Q}(k)]$ is the pdf of the random matrix $\mathbb{Q}(k)$, and the second equality is derived by substituting (29) into (30). Furthermore, the probability mass function $P(K=k)$ is derived as

$$\begin{aligned}P(K=k)&=P(K>k-1)-P(K>k)\\&=\overrightarrow{\boldsymbol{\tau}}\overline{\mathbf{Q}}^{k-1}\overrightarrow{\mathbf{1}}-\overrightarrow{\boldsymbol{\tau}}\overline{\mathbf{Q}}^{k}\overrightarrow{\mathbf{1}}\\&=\overrightarrow{\boldsymbol{\tau}}(\overline{\mathbf{Q}}^{k-1}-\overline{\mathbf{Q}}^{k})\overrightarrow{\mathbf{1}}=\overrightarrow{\boldsymbol{\tau}}\overline{\mathbf{Q}}^{k-1}(\mathbf{I}-\overline{\mathbf{Q}})\overrightarrow{\mathbf{1}}\\&=\overrightarrow{\boldsymbol{\tau}}\overline{\mathbf{Q}}^{k-1}\overline{\mathbf{Q}}_{0}\end{aligned} \tag{31}$$

where $\overline{\mathbf{Q}}_0$ is the expected vector of $\mathbf{Q}_0(t)$ defined in (26).

To obtain the expected value of the random content dissemination delay K, Theorem 3 is formulated as follows.

Theorem 3: The ijth entry θ_{ij} of the new matrix $\boldsymbol{\Theta}=\sum_{k=0}^{\infty}\mathbb{Q}(k)$ represents the expected number of frames that the DT-PBMC spends in state j, given the initial state i.

Proof: See Appendix C. ■

Given Theorem 3, after summing up all the entries in row i of matrix $\boldsymbol{\Theta}$, we have the expected number of frames that the DT-PBMC spends in the transient states, which is also the expected number of frames before the DT-PBMC is terminated. Therefore, we have

$$E\left[K|\left\{\mathbb{Q}(k)|k=0,1,\ldots,+\infty\right\}\right]=\overrightarrow{\boldsymbol{\tau}}\boldsymbol{\Theta}\overrightarrow{\mathbf{1}}=\overrightarrow{\boldsymbol{\tau}}\sum_{k=0}^{\infty}\mathbb{Q}(k)\overrightarrow{\mathbf{1}} \tag{32}$$

where $\overrightarrow{\boldsymbol{\tau}}$ and $\overrightarrow{\mathbf{1}}$ have already been defined in (29). Furthermore, according to the Bayesian principle and Theorem 2, we have

$$\begin{aligned}E[K]&=\overrightarrow{\boldsymbol{\tau}}\left[\sum_{k=0}^{\infty}\int_{\mathbb{Q}(k)}\mathbb{Q}(k)f\left[\mathbb{Q}(k)\right]d\mathbb{Q}(k)\right]\overrightarrow{\mathbf{1}}\\&=\overrightarrow{\boldsymbol{\tau}}\times\sum_{k=0}^{\infty}E\left[\mathbb{Q}(k)\right]\times\overrightarrow{\mathbf{1}}\\&=\overrightarrow{\boldsymbol{\tau}}\times\sum_{k=0}^{\infty}\overline{\mathbf{Q}}^{k}\times\overrightarrow{\mathbf{1}}\end{aligned} \tag{33}$$

where $f[\mathbb{Q}(k)]$ is the pdf of the random matrix $\mathbb{Q}(k)$. For the sake of deriving the closed-form expression of $\sum_{k=0}^{\infty}\overline{\mathbf{Q}}^{k}$, the following theorem is formulated.

Theorem 4: The inverse matrix of $(\mathbf{I}-\overline{\mathbf{Q}})$ exists, and $\sum_{k=0}^{\infty}\overline{\mathbf{Q}}^{k}=(\mathbf{I}-\overline{\mathbf{Q}})^{-1}$.

Proof: See Appendix D. ■

Finally, according to Theorem 4, we arrive at the closed-form expression of the expected number of frames that the DT-PBMC encountered before being terminated, which is also the average content dissemination delay of

$$E[K]=\overrightarrow{\boldsymbol{\tau}}\times\sum_{k=0}^{\infty}\overline{\mathbf{Q}}^{k}\times\overrightarrow{\mathbf{1}}=\overrightarrow{\boldsymbol{\tau}}(\mathbf{I}-\overline{\mathbf{Q}})^{-1}\overrightarrow{\mathbf{1}}. \tag{34}$$

V. Numerical Results

The power spectral density of the noise is $N_0=-174$ dBm/Hz, and the bandwidth for the COs' social multicast is $W=10$ MHz. Hence, the noise power is $N_0W=-104$ dBm. If the transmission from a CO to CSs takes place at the carrier frequency of 3.6 GHz, the PL at the reference point stipulated to be $d_0=1$ m away from the transmitter is 44 dB, according to the free-space PL equation [31], whereas the PL exponent for the receiver beyond d_0 is set to be $\kappa=3$. Furthermore, we generally set the received power at the reference point to be $P_0=-34$ dBm. This setting indicates that the actual transmit power is 10 dBm ($=-34$ dBm $+44$ dB). We also set the successful packet reception SNR threshold to be $\gamma=10$ dB, which guarantees that the BER at the receiver is below 10^{-2} without channel coding [37]. All these physical-layer-related parameter settings are in line with the 802.11 protocol [38]. All the MSs roam in the bounded circular area having a radius of $R=50$ m by obeying the mobility model

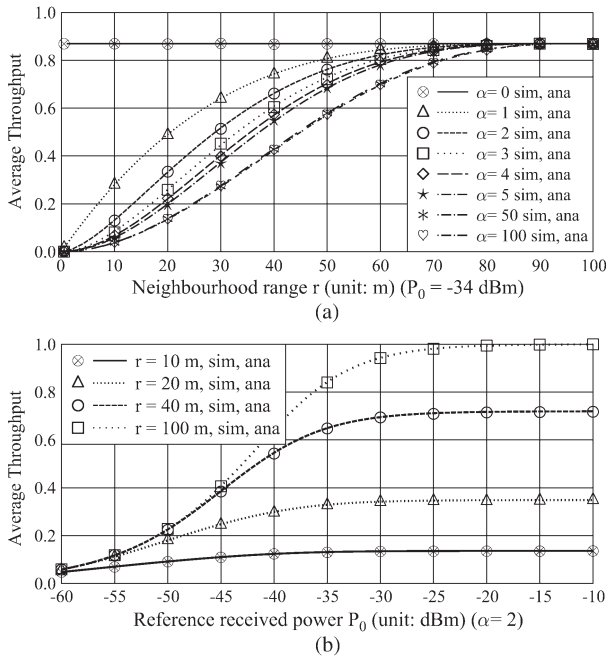

Fig. 8. Average social unicast throughput. (a) Neighbourhood range. (b) Reference received power.

introduced in Section III-C. To accurately characterize the statistical properties of the system, we repeated the content dissemination process corresponding to the model introduced in Section II 100 000 times.

To obtain accurate analytical results, we set $n_{\max}$ in $\widetilde{f_Y}(y)$ of (9) to be $n_{\max} = 10$. According to Fig. 5, when $R = 50$ m, the RMSE between $\widetilde{f_Y}(y)$ of (9) and $f_Y(y)$ of (4) is 3×10^{-5}.

A. Social Unicast Throughput

We first vary the neighborhood range r from 1 to 100 m and then increase the social exponent α from 0 to 100. The impact of r and α on the average social unicast throughput is evaluated.

In Fig. 8(a), we observe that as the neighborhood range r increases, the average social unicast throughput remains constant for $\alpha = 0$. In this case, based on (1), the CS may become the CO's opportunistic contact with a unity probability. As a result, increasing r does not affect the social unicast throughput. However, if $\alpha \neq 0$, we may observe in Fig. 8(a) that the average social unicast throughput increases as we increase the neighborhood range r. This can be explained by the fact that a higher neighborhood range increases the probability of the CS becoming one of the CO's social contacts, as shown in (1). Furthermore, if r is equal to the maximum possible distance $2R$ in a circular area, observe in Fig. 8(a) that the average throughput achieves its maximum value for $\alpha = 0$, because in this case, the destination is always one of the source's regular contacts. Moreover, since a higher α indicates that the CS may become one of the CO's opportunistic contact with a lower probability, it is less likely to establish a physical wireless link between the CO and the CS beyond the CO's neighborhood range. As a result, a higher α leads to a reduced average throughput. Furthermore, in the case of α tending to infinity, the CO is only willing to share the content with the CSs within his/her neighborhood range. Hence, we observe in Fig. 8(a) that if α is high, e.g., 50 or 100, the average social unicast throughput converges to that of the scenario where communications between a CS and CO pair only occur if the CS is within the CO's neighborhood range.

Then, we set $\alpha = 2$, and vary the reference received power P_0 from -60 to -10 dBm in combination with different neighborhood ranges r. Observe in Fig. 8(b) that the average social unicast throughput increases as we increase P_0. However, the average social unicast throughput converges to a constant value, as P_0 tends to infinity. According to our analysis in Section III-D, the social unicast throughput depends both on the successful packet delivery probability $\nu|_{Y=y}$ of a physical wireless link and on the geographic social strength $\varphi|_{Y=y}$. When the transmit power tends to infinity, $\nu|_{Y=y}$ converges to one; hence, the average social unicast throughput is dominated by the geographic social strength $\varphi|_{Y=y}$. As a result, when we have $r = 100$ m, indicating no influence from the geographic social strength, the average throughput converges to one. However, when r is below 100 m, the average social unicast throughput converges to a specific value, which is derived by integrating the social strength $\varphi|_{Y=y}$ over the distance pdf $f_Y(y)$.

B. Content Dissemination Delay

Let us fix the neighborhood range to $r = 10$ m and fix the social exponent to $\alpha = 3$, whereas the number of COs initially receiving the content before the content dissemination process is set to be $U = 5$. The other physical-layer-related parameters are the same as the parameters introduced at the beginning of Section V.

In Fig. 9(a), we evaluate the average content dissemination delay of four different protocols. We observe in Fig. 9(a) that both the "Noncoop direct so-multicast" and "Single-stage coop so-multicast" protocols exhibit a monotonically increasing trend in terms of the average content dissemination delay, as we increase the number of MSs in the bounded circular area. Since the served CSs join the initial group of COs for further forwarding the content of common interest, we observe in Fig. 9(a) that the average content dissemination delay is significantly reduced when the "Noncoop gossip so-multicast" protocol is invoked. Our "multistage coop so-multicast" protocol is capable of further reducing the average content dissemination delay, because our social multicast procedure provides more successful content delivery opportunities than social unicast. Based on this comparison, we conclude that our multistage cooperative social multicast protocol is significantly faster in disseminating the content of common interest than the other three existing protocols, when imposing social constraint on the wireless transmissions.

As evidenced by Fig. 9(b), we observe that the content dissemination delay converges to two frames under our protocol. More explicitly, as we increase the number of MSs to $N = 600$, we observe in Fig. 9(b) that both our simulation and analytical results of the average content dissemination delay finally converge to two frames, regardless of the value of the social exponent α. This somewhat surprising results suggest that when there are sufficient MSs in the circular area, invoking two-stage cooperative social multicast is sufficient

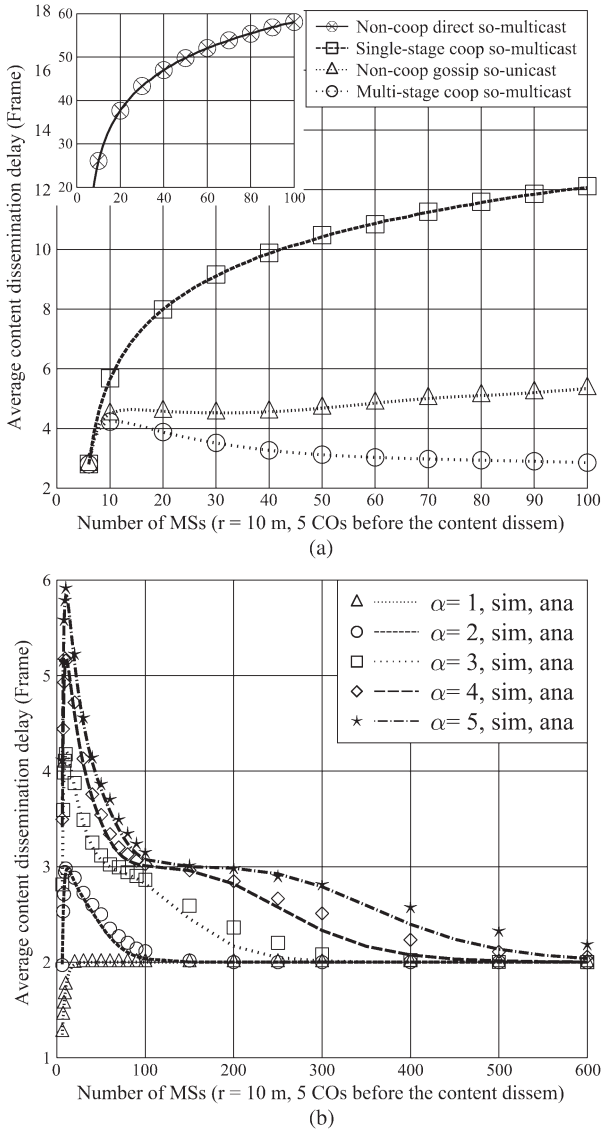

Fig. 9. Impact of the number of MSs on the content dissemination delay. (a) Comparison. (b) Convergence.

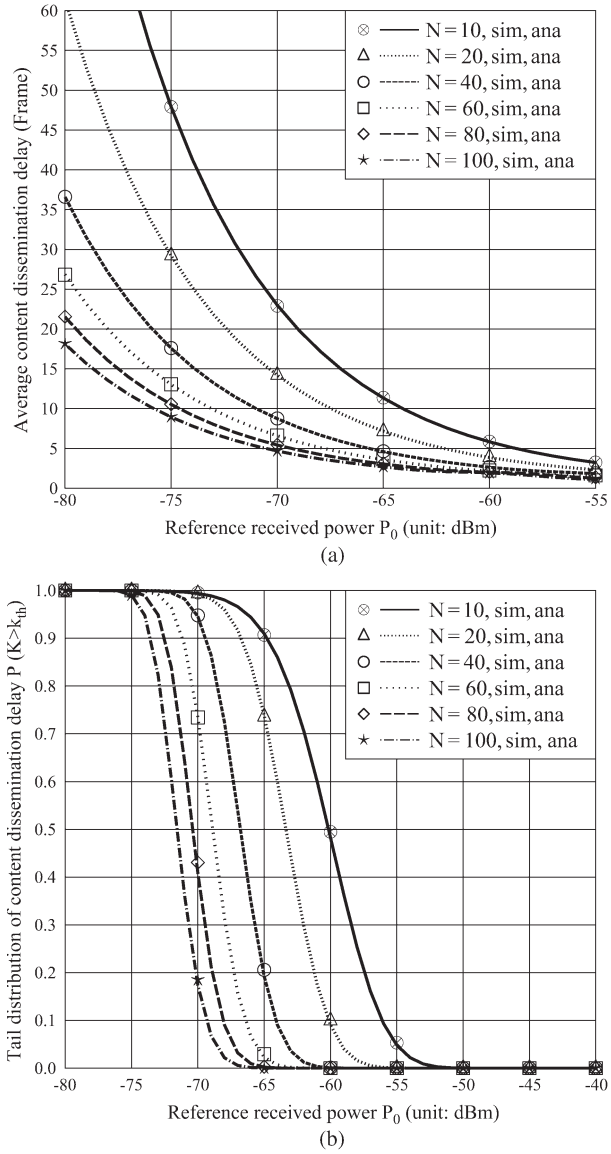

Fig. 10. Impact of the reference received power on the content dissemination delay. (a) Average delay. (b) Tail distribution.

on average for the sake of guaranteeing that all the interested MSs successfully receive the content. Furthermore, according to our simulations, for $\alpha = 5, 4, 3$, and 2, the specific number of MSs, resulting in the highest average content dissemination delay, is 10, 11, 11, and 12, respectively. As a result, we may conclude that a higher α results in an early reduction of the content dissemination delay. However, when $\alpha = 1$, the content dissemination delay increases and finally converges to two frames, because in contrast to the other scenarios, the delay is lower than two frames, when N is smaller.

Finally, we set the social exponent α to $\alpha = 0$ for the sake of canceling the impact of the socially related parameters and vary the reference received power P_0 from -80 to -55 dBm. Half of the MSs are assumed to receive the content of common interest before the content dissemination process. During each frame, the COs multicast the content to all CSs rather than only multicast the content to his/her social contacts. As a result, the physical-layer parameters dominate the attainable content dissemination performance.

We may observe in Fig. 10(a) that the average content dissemination delay substantially reduces as we increase P_0. For the case of $N = 40$, the average content dissemination delay reduces from 37 frames at $P_0 = -80$ dBm to just one frame at $P_0 = -55$ dBm. Furthermore, in Fig. 10(b), we evaluate the probability of the content dissemination delay exceeding a predefined threshold of $k_{\rm th} = 5$ frames. Observe in Fig. 10(b) that the tail probability of the content dissemination delay decreases as we increase P_0.

VI. Conclusion and Discussions

In this paper, we have proposed a distributed multistage cooperative-social-multicast-protocol-aided content dissemination scheme. According to our research, several important conclusions may be drawn.

i) Both the social unicast throughput and the content dissemination delay are heavily affected by both the social

parameters and the physical-layer parameters. Both a more communicative CO, which is represented by a lower social exponent α, and a higher neighborhood range r substantially increase the social unicast throughput and reduce the content dissemination delay. Similarly, a more powerful transceiver, which is represented by a higher reference received power P_0, and a lower successful packet reception SNR threshold γ have the same beneficial effects.

ii) The content dissemination delay is also heavily affected by the number of interested MSs. An increased number of interested MSs provides more potential COs during the content dissemination process. Since every CO is willing to multicast the content of common interest to CSs, this diversity gain provided by multiple COs is capable of substantially reducing the content dissemination delay. When the number of interested MSs is high, using two-stage cooperative social multicast is sufficient for the sake of guaranteeing that all the MSs successfully receive the content of common interest.

iii) As demonstrated by the numerical results, our multistage cooperative social multicast protocol outperforms the other three existing protocols in terms of its average content dissemination delay, including the noncooperative direct social multicast protocol, the single-stage cooperative social multicast protocol, and the noncooperative gossip-based social unicast protocol. Our protocol is more suitable than the other three, when the geographic social relationships are taken into consideration.

Furthermore, our analytical model invoked for analyzing the delay of the content dissemination has wide-ranging applications.

i) If we set the social exponent to $\alpha = 0$ or set the neighborhood range to $r = 2R$, the impact of the social parameters is eliminated. Hence, our analytical model can be invoked for analyzing both the delay and the throughput of the conventional multistage cooperative multicast technique.

ii) If we set the social exponent to $\alpha = +\infty$ and equate the neighborhood range to the transmission range, our analytical model can also be used for analyzing the delay characteristics of the mobile ad hoc networks [39]. In this scenario, a packet can only be received by a CS, when it roams within the CO's transmission range and when the wireless link is capable of successfully delivering the content.

iii) Our analytical model can also be used for analyzing the content dissemination delay for the noncooperative social multicast protocol. Since only a single CO is multicasting the content during a transmission frame, we simply set $n = 1$ in (24) for the sake of characterizing the delay performance of this protocol.

iv) Our analytical model can also be used for analyzing the content dissemination delay for the single-stage cooperative social multicast protocol. Given this protocol, only the initial group of COs, whose size is U, cooperatively social multicast the content of common interest. Hence, if we set $n = U$ in (24), we may readily derive the delay characteristics of this protocol.

APPENDIX A
PROOF OF THEOREM 1

This theorem may be proved by using the technique of mathematical induction.

Explicitly, when we have $k = 0$, $\mathbb{Q}(0) = \mathbf{Q}(0) = I$, and the theorem holds, because the system stays at its current state after 0 frames with a unity probability.

When $k = 1$, $\mathbb{Q}(1) = \mathbf{Q}(0)\mathbf{Q}(1) = I \times \mathbf{Q}(1) = \mathbf{Q}(1)$. The ijth entry of $\mathbb{Q}(1)$ is $q_{ij}(1) = p_{ij}(1)$. Since $p_{ij}(1)$ is the transition probability from state i to state j during frame 1, it is also the probability of state j being reached after one frame, given the initial state i.

Furthermore, we assume that Theorem 1 holds for $\mathbb{Q}(k) = \prod_{t=0}^{k} \mathbf{Q}(t)$, whose ijth entry is $q_{ij}(k)$. Then, the probability of state j being reached after $(k+1)$ frames, given the initial state i, is derived as

$$q_{ij}(k+1) = \sum_{h=i}^{j} q_{ih}(k) p_{hj}(k+1),\ i \le j. \tag{35}$$

Thus, matrix $\mathbb{Q}(k+1)$ constructed by $q_{ij}(k+1)$ can be also expressed as $\mathbb{Q}(k+1) = \mathbb{Q}(k)\mathbf{Q}(k+1) = \prod_{t=0}^{k+1} \mathbf{Q}(t)$. Hence, Theorem 1 is proved.

APPENDIX B
PROOF OF THEOREM 2

Given the initial state i and the ijth entry $q_{ij}(k+1)$ of $\mathbb{Q}(k+1)$ in (35), the probability of the DT-PBMC not being terminated after $(k+1)$ frames can be expressed as the sum of the ith row's entries, which is formulated as

$$\begin{aligned} p_{i,unab}(k+1) &= \sum_{j=1}^{N-1} q_{ij}(k+1) = \sum_{j=i}^{N-1} \sum_{h=i}^{j} q_{ih}(k) p_{hj}(k+1) \\ &= \sum_{j=i}^{N-1} q_{ij}(k)[p_{j,1}(k+1) + \cdots + p_{j,N-1}(k+1)] \\ &= \sum_{j=i}^{N-1} q_{ij}(k)\left[1 - p_{j,N}(k+1)\right]. \end{aligned} \tag{36}$$

Clearly, the probability of the DT-PBMC not being terminated after k frames is expressed as

$$p_{i,unab}(k) = \sum_{j=i}^{N-1} q_{ij}(k). \tag{37}$$

Since $0 \le p_{j,N} \le 1$, we have $p_{i,unba}(k+1) < p_{i,unba}(k)$. Obviously, the probability of the DT-PBMC not being terminated is a monotonically decreasing function with respect to the number of frames k. If k tends to infinity, we may have

$$\lim_{k\to\infty} p_{i,unab}(k) = \lim_{k\to\infty} \sum_{j=i}^{N-1} q_{ij}(k) = 0. \tag{38}$$

Thus, the relation of $\lim_{k\to\infty} q_{ij}(k) = 0$ can be inferred. As a result, we have $\lim_{k\to\infty} \mathbb{Q}(k) = \mathbf{0}$. Furthermore, since the set

of $\{\mathbf{Q}(t), t = 0, 1, 2, \ldots\}$ consists of i.i.d. random matrices, we have

$$\lim_{k\to\infty} E\left[\mathbb{Q}(k)\right] = \lim_{k\to\infty} \prod_{t=0}^{k} E\left[\mathbf{Q}(t)\right] = \lim_{k\to\infty} \overline{\mathbf{Q}}^{k} = 0. \quad (39)$$

Hence, Theorem 2 is proved.

Appendix C
Proof of Theorem 3

According to Theorem 1, the ijth entry $q_{ij}(k)$ of $\mathbb{Q}(k)$ represents the probability of transient state j being reached after k frames, given the initial state i. Then, given the initial state i, a new random variable $X(k)$ is defined. It is 1 if state j is reached after k frames, and it is 0 otherwise. Hence, we have $P[X(k) = 1] = q_{ij}(k)$ and $P[X(k) = 0] = 1 - q_{ij}(k)$. Then, the expected value of $X(k)$ is $E[X(k)] = q_{ij}(k)$.

When considering the transmission of k frames, state j may be reached at any frame index spanning from zero to k. Hence, the total number of times that state j is reached during these k frames can be expressed as $X(0) + X(1) + \cdots + X(k)$, whose expected value is

$$E[X(0)+X(1)+\cdots+X(k)]=q_{ij}(0)+q_{ij}(1)+\cdots+q_{ij}(k).$$

If k tends to infinity, we have

$$E\left[X(0) + X(1) + \cdots\right] = q_{ij}(0) + q_{ij}(1) + \cdots = \theta_{ij}. \quad (40)$$

If we expand (40) to a matrix form, we arrive at $\mathbf{\Theta} = \sum_{k=0}^{\infty} \mathbb{Q}(k)$, whose ijth entry is θ_{ij}.

Since the time elapse is measured in terms of the number of frames in the DT-PBMC, given the initial state i, transient state j is reached θ_{ij} times on average, which indicates that the system stays in state j for θ_{ij} frames on average. Hence, Theorem 3 is proved.

Appendix D
Proof of Theorem 4

Let us construct a system of linear equations $(I - \overline{\mathbf{Q}})\overrightarrow{\mathbf{x}} = \mathbf{0}$, where $\overrightarrow{\mathbf{x}}$ is a $1 \times (N-1)$-element column vector. Then, iterating this equation k times, we have $\overrightarrow{\mathbf{x}} = \overline{\mathbf{Q}}^{k}\overrightarrow{\mathbf{x}}$. Upon letting k to tend to infinity, according to Theorem 2, we have $\lim_{k\to\infty} \overline{\mathbf{Q}}^{k} = \mathbf{0}$. Then, the equation $(I - \overline{\mathbf{Q}})\overrightarrow{\mathbf{x}} = \mathbf{0}$ has a single solution, which is $\overrightarrow{\mathbf{x}} = \overrightarrow{\mathbf{0}}$. Hence, we may claim that $(\mathbf{I} - \overline{\mathbf{Q}})$ is a full-rank square matrix, whose inverse matrix denoted by $(\mathbf{I} - \overline{\mathbf{Q}})^{-1}$ does exist.

Clearly, the following equation holds:

$$(\mathbf{I} - \overline{\mathbf{Q}}) \times (\mathbf{I} + \overline{\mathbf{Q}} + \overline{\mathbf{Q}}^{2} + \cdots + \overline{\mathbf{Q}}^{k}) = \mathbf{I} - \overline{\mathbf{Q}}^{k+1}. \quad (41)$$

Left-multiplying both sides of (41) by $(\mathbf{I} - \overline{\mathbf{Q}})^{-1}$, we arrive at

$$\mathbf{I} + \overline{\mathbf{Q}} + \overline{\mathbf{Q}}^{2} + \cdots + \overline{\mathbf{Q}}^{k} = (\mathbf{I} - \overline{\mathbf{Q}})^{-1} \times (\mathbf{I} - \overline{\mathbf{Q}}^{k+1}). \quad (42)$$

Provided that $\lim_{k\to\infty} \overline{\mathbf{Q}}^{k} = \mathbf{0}$ holds, upon letting k in both sides tend to infinity, we have

$$\sum_{k=0}^{\infty} \overline{\mathbf{Q}}^{k} = (\mathbf{I} - \overline{\mathbf{Q}})^{-1}. \quad (43)$$

Hence, Theorem 4 is proved.

References

[1] S.-J. Lee, W. Su, and M. Gerla, "On-demand multicast routing protocol in multihop wireless mobile networks," *Mobile Netw. Appl.*, vol. 7, no. 6, pp. 441–453, Dec. 2002.

[2] J. Wang, S. Park, D. Love, and M. Zoltowski, "Throughput delay trade-off for wireless multicast using hybrid-ARQ protocols," *IEEE Trans. Commun.*, vol. 58, no. 9, pp. 2741–2751, Sep. 2010.

[3] C.-H. Liu and J. Andrews, "Multicast outage probability and transmission capacity of multihop wireless networks," *IEEE Trans. Inf. Theory*, vol. 57, no. 7, pp. 4344–4358, Jul. 2011.

[4] B. Niu, H. Jiang, and H. Zhao, "A cooperative multicast strategy in wireless networks," *IEEE Trans. Veh. Technol.*, vol. 59, no. 6, pp. 3136–3143, Jul. 2010.

[5] J.-H. Wui and D. Kim, "Optimal power allocation between unicast and multicast messages in wireless relay-multicasting networks using superposition coding," *IEEE Commun. Lett.*, vol. 15, no. 11, pp. 1159–1161, Nov. 2011.

[6] I.-H. Lee, H. Lee, and H.-H. Choi, "Exact outage probability of relay selection in decode-and-forward based cooperative multicast systems," *IEEE Commun. Lett.*, vol. 17, no. 3, pp. 483–486, Mar. 2013.

[7] Y. Zhou *et al.*, "Two-stage cooperative multicast transmission with optimized power consumption and guaranteed coverage," *IEEE J. Sel. Areas Commun.*, vol. 32, no. 2, pp. 274–284, Feb. 2014.

[8] H. Zhao and W. Su, "Cooperative wireless multicast: Performance analysis and power location optimization," *IEEE Trans. Wireless Commun.*, vol. 9, no. 6, pp. 2088–2100, Jun. 2010.

[9] J.-B. Seo, T. Kwon, and V. Leung, "Social Groupcasting algorithm for wireless cellular multicast services," *IEEE Commun. Lett.*, vol. 17, no. 1, pp. 47–50, Jan. 2013.

[10] N. Kayastha, D. Niyato, P. Wang, and E. Hossain, "Applications, architectures, protocol design issues for mobile social networks: A survey," *Proc. IEEE*, vol. 99, no. 12, pp. 2130–2158, Dec. 2011.

[11] C. Xu, S. Jia, L. Zhong, H. Zhang, and G. Muntean, "Ant-inspired mini-community-based solution for video-on-demand services in wireless mobile networks," *IEEE Trans. Broadcast.*, vol. 60, no. 2, pp. 322–335, Jun. 2014.

[12] C. Xu *et al.*, "Performance-aware mobile community-based VoD streaming over vehicular *Ad Hoc* networks," *IEEE Trans. Veh. Technol.*, to be published. AQ1

[13] K.-J. Lin, C.-W. Chen, and C.-F. Chou, "Preference-aware content dissemination in opportunistic mobile social networks," in *Proc. IEEE INFOCOM*, Mar. 2012, pp. 1960–1968.

[14] P. TalebiFard and V. C. Leung, "A content centric approach to dissemination of information in vehicular networks," in *Proc. 2nd ACM Int. Symp. Design Anal. Intell. Veh. Netw. Appl., ser. DIVANet'12*, 2012, pp. 17–24. [Online]. Available: http://doi.acm.org/10.1145/2386958.2386962

[15] S. Bastani, B. Landfeldt, C. Rohner, and P. Gunningberg, "A social node model for realising information dissemination strategies in delay tolerant networks," in *Proc. 15th ACM Int. Conf. Model., Anal. Simul. Wireless Mobile Syst., ser. MSWiM'12*, 2012, pp. 79–88. [Online]. Available: http://doi.acm.org/10.1145/2387238.2387254

[16] Y. Li *et al.*, "The impact of node selfishness on multicasting in delay tolerant networks," *IEEE Trans. Veh. Technol.*, vol. 60, no. 5, pp. 2224–2238, Jun. 2011.

[17] J. Hu, L.-L. Yang, and L. Hanzo, "Mobile social networking aided content dissemination in heterogeneous networks," *China Commun.*, vol. 10, no. 6, p. 1, Jun. 2013. [Online]. Available: http://www.chinacommunications.cn/EN/abstract/article_8138.shtml

[18] V. Sevani, B. Raman, and P. Joshi, "Implementation-based evaluation of a full-fledged multihop TDMA-MAC for WiFi mesh networks," *IEEE Trans. Mobile Comput.*, vol. 13, no. 2, pp. 392–406, Feb. 2014.

[19] J. Hu, L.-L. Yang, and L. Hanzo, "Throughput and delay analysis of wireless multicast in distributed mobile social networks based on geographic social relationships," in *Proc. IEEE WCNC*, Apr. 2014, pp. 1–6. [Online]. Available: http://eprints.soton.ac.uk/362323/

[20] A. Dimakis, S. Kar, J. Moura, M. Rabbat, and A. Scaglione, "Gossip algorithms for distributed signal processing," *Proc. IEEE*, vol. 98, no. 11, pp. 1847–1864, Nov. 2010.

[21] H. Zhang, Z. Zhang, and H. Dai, "Gossip-based information spreading in mobile networks," *IEEE Trans. Wireless Commun.*, vol. 12, no. 11, pp. 5918–5928, Nov. 2013.

[22] J. Travers, S. Milgram, J. Travers, and S. Milgram, "An experimental study of the small world problem," *Sociometry*, vol. 32, no. 4, pp. 425–443, Dec. 1969.

[23] D. J. Watts and S. H. Strogatz, "Collective dynamics of 'small-world' networks," *Nature*, vol. 393, no. 6684, pp. 440–442, Jun. 1998.

[24] H. Inaltekin, M. Chiang, and H. V. Poor, "Average message delivery time for small-world networks in the continuum limit," *IEEE Trans. Inf. Theory*, vol. 56, no. 9, pp. 4447–4470, Sep. 2010.
[25] H. Inaltekin, M. Chiang, and H. V. Poor, "Delay of social search on small-world graphs," *J. Math. Sociol.*, vol. 38, no. 1, pp. 1–45, Sep. 2013.
[26] J. Kleinberg, "The small-world phenomenon: An algorithm perspective," in *Proc. 32nd Annu. ACM Symp. Theory Comput.*, *ser. STOC'00*, 2000, pp. 163–170.
[27] B. Azimdoost, H. Sadjadpour, and J. Garcia-Luna-Aceves, "The impact of social groups on the capacity of wireless networks," in *Proc. IEEE NSW*, Jun. 2011, pp. 30–37.
[28] D. Liben-Nowell, J. Novak, R. Kumar, P. Raghavan, and A. Tomkins, "Geographic routing in social networks," *Proc. Nat. Academy Sci. USA*, vol. 102, no. 33, pp. 11 623–11 628, Aug. 2005.
[29] J.-P. Onnela, S. Arbesman, M. C. González, A.-L. Barabási, and N. A. Christakis, "Geographic constraints on social network groups," PLoS One, vol. 6, no. 4, p. 1, Apr. 2011. [Online]. Available: http://arxiv.org/abs/1011.4859. [Online]. Available: http://arxiv.org/abs/1011.4859
[30] A. Clauset, C. R. Shalizi, and M. E. J. Newman, "Power-law distributions in empirical data," *SIAM Rev.*, vol. 51, no. 4, pp. 661–703, Nov. 2009. [Online]. Available: http://dx.doi.org/10.1137/070710111
[31] T. Rappaport, *Wireless Communications: Principles and Practice*, 2nd ed. Upper Saddle River, NJ, USA: Prentice-Hall, 2001.
[32] J. Hu, L. Yang, and L. Hanzo, "Maximum average service rate and queue scheduling and performance analysis of delay-constrained hybrid cognitive radio in Nakagami channels," *IEEE Trans. Veh. Technol.*, vol. 62, no. 5, pp. 2220–2229, Jun. 2013.
[33] J. Hu, L.-L. Yang, and L. Hanzo, "Optimal queue scheduling for hybrid cognitive radio maintaining maximum average service rate under delay constraints," in *Proc. IEEE GLOBECOM*, 2012, pp. 1398–1403.
[34] M. Grossglauser and D. Tse, "Mobility increases the capacity of *ad hoc* wireless networks," *IEEE/ACM Trans. Netw.*, vol. 10, no. 4, pp. 477–486, Aug. 2002.
[35] C. Bettstetter, H. Hartenstein, and X. Pérez-Costa, "Stochastic properties of the random waypoint mobility model," *Wireless Netw.*, vol. 10, no. 5, pp. 555–567, Sep. 2004. [Online]. Available: http://dx.doi.org/10.1023/B:WINE.0000036458.88990.e5
[36] I. S. Gradshteyn and I. M. Ryzhik, *Table of Integrals, Series, Products*, 7th ed. Amsterdam, The Netherlands: Academic, 2007, Elsevier.
[37] L.-L. Yang, *Multicarrier Communication*, 1st ed. Hoboken, NJ, USA: Wiley, 2009.
[38] *Information Technology—Telecommunications and Information Exchange Between Systems Local and Metropolitan Area Networks—Specific Requirements Part 11: Wireless LAN Medium Access Control (MAC) and Physical Layer (PHY) Specifications*, ISO/IEC/IEEE 8802-11:2012(E), Nov. 2012, pp. 1–2798.
[39] L. Hanzo and R. Tafazolli, "A survey of QoS routing solutions for mobile *ad hoc* networks," *IEEE Commun. Surveys Tuts.*, vol. 9, no. 2, pp. 50–70, 2007.

Jie Hu (S'11) received the B.Eng. degree in communication engineering and the M.Eng. degree in communication and information system from the School of Communication and Information Engineering, Beijing University of Posts and Telecommunications, Beijing, China, in 2008 and 2011, respectively. He is currently working toward the Ph.D. degree with the Communication, Signal Processing and Control Group, University of Southampton, Southampton, U.K.

His research interests in wireless communications include cognitive radio and cognitive networks, queuing analysis, resource allocation and scheduling, ad hoc wireless networks, and mobile social networks.

Lie-Liang Yang (M'98–SM'02) received the B.Eng. degree in communications engineering from Shanghai TieDao University, Shanghai, China, in 1988 and the M.Eng. and Ph.D. degrees in communications and electronics from Beijing Jiaotong University, Beijing, China, in 1991 and 1997, respectively.

From June 1997 to December 1997, he was a Visiting Scientist with the Institute of Radio Engineering and Electronics, Academy of Sciences of the Czech Republic, Prague, Czech Republic. Since December 1997, he has been with the University of Southampton, Southampton, U.K., where he is a Professor of wireless communications with the School of Electronics and Computer Science. He has published over 300 research papers in journals and conference proceedings and several book chapters and has authored/coauthored three books. (The details about his publications can be found at http://www-mobile.ecs.soton.ac.uk/lly/.) His research has covered a wide range of topics in wireless communications, networking, and signal processing.

Dr. Yang is a Fellow of the Institution of Engineering and Technology, served as an Associate Editor for the IEEE TRANSACTIONS ON VEHICULAR TECHNOLOGY and the *Journal of Communications and Networks*, and is currently an Associate Editor of the IEEE ACCESS and the *Security and Communication Networks Journal*.

Lajos Hanzo (F'08) received the M.S. degree in electronics and the Ph.D. degree from Budapest University of Technology and Economics (formerly, Technical University of Budapest), Budapest, Hungary, in 1976 and 1983, respectively; the D.Sc. degree from the University of Southampton, Southampton, U.K., in 2004; and the "Doctor Honoris Causa" degree from Budapest University of Technology and Economics in 2009.

During his 38-year career in telecommunications, he has held various research and academic posts in Hungary, Germany, and the U.K. Since 1986, he has been with the School of Electronics and Computer Science, University of Southampton, where he holds the Chair in Telecommunications. He is currently directing a 100-strong academic research team, working on a range of research projects in the field of wireless multimedia communications sponsored by industry, the Engineering and Physical Sciences Research Council of U.K., the European Research Council's Advanced Fellow Grant, and the Royal Society Wolfson Research Merit Award. During 2008–2012, he was a Chaired Professor with Tsinghua University, Beijing, China. He is an enthusiastic supporter of industrial and academic liaison and offers a range of industrial courses. He has successfully supervised more than 80 Ph.D. students, coauthored 20 John Wiley/IEEE Press books on mobile radio communications totaling in excess of 10 000 pages, and published more than 1400 research entries on IEEE Xplore. He has more than 20 000 citations. His research is funded by the European Research Council's Senior Research Fellow Grant. (For further information on research in progress and associated publications, please see http://www-mobile.ecs.soton.ac.uk.)

Dr. Hanzo is a Fellow of the Royal Academy of Engineering, The Institution of Engineering and Technology, and the European Association for Signal Processing. He is also a Governor of the IEEE Vehicular Technology Society. He has served as the Technical Program Committee Chair and the General Chair of IEEE conferences, has presented keynote lectures, and has received a number of distinctions. During 2008–2012, he was the Editor-in-Chief of the IEEE Press.

AUTHOR QUERIES

AUTHOR PLEASE ANSWER ALL QUERIES

AQ1 = Please provide publication update in Ref. [12].

END OF ALL QUERIES